METROLOGY AND MEASUREMENT SYSTEMS 3D MODELLING OF CYLINDRICAL-SHAPED OBJECTS FROM LIDAR D....

Article *in* Metrology and Measurement Systems · March 2018

DOI: 10.24425/118156

CITATIONS

0

3 authors, including:

Jakub Szulwic

Gdansk University of Technology

126 PUBLICATIONS **459** CITATIONS

SEE PROFILE

Metrol. Meas. Syst., Vol. 25 (2018) No. 1, pp. 47–56.

PAN POLSKA AKADEMIA NAUK

METROLOGY AND MEASUREMENT SYSTEMS

Index 330930, ISSN 0860-8229

www.metrology.pg.gda.pl

M&MS

3D MODELLING OF CYLINDRICAL-SHAPED OBJECTS FROM LIDAR DATA – AN ASSESSMENT BASED ON THEORETICAL MODELLING AND EXPERIMENTAL DATA

Artur Janowski[1)], Katarzyna Bobkowska[2)], Jakub Szulwic[2)]

1) *University of Warmia and Mazury in Olsztyn, Faculty of Geodesy, Geospatial and Civil Engineering, M. Oczapowskiego 2, 10-719 Olsztyn, Poland* (*artur.janowski@geodezja.pl*)

2) *Gdańsk University of Technology, Faculty of Civil and Environmental Engineering, G. Narutowicza 11/12, 80-233 Gdańsk, Poland* (*katbobko@pg.edu.pl*, ✉ *jakub.szulwic@pg.edu.pl*, +48 58 347 1012)

Abstract

Despite the increasing availability of measured laser scanning data and their widespread use, there is still the problem of rapid and correct numerical interpretation of results. This is due to the large number of observations that carry similar information. Therefore, it is necessary to extract from the results only the essential features of the modelled objects. Usually, it is based on a process using filtration, followed by simplification and generalization of redundant contents of datasets. This process must ensure the collection of new data without loss of information contained therein, the description accuracy of the key features of a measured object, as well as the uniqueness and comparability of results. In this paper, the authors extend the already extensive range of algorithms for the automatic or semiautomatic modelling of cylindrical objects, which have been measured using the laser scanning technology, with the one employing a concave hull or – in general – the alpha-shape (α-shape).

The applicability of the proposed method was analysed using simulated data – generated analytically with the introduced and established systematic error with normal distribution – and using real results of the measurement of cylindrical-shaped objects. For real data, the obtained results were compared with the reference data. This made it possible to determine the validity of the proposed new method.

Keywords: α-shape, 2D Delaunay triangulation, 3D modelling, laser measurements, silo measurements.

1. Introduction

Effective modelling of structures engineered using the-state-of-the-art measurement methods is related to the increasing accuracy of observations and their huge numbers. Often the number of measurement samples describing a modelled space is so large that its oversize (though giving an increased level of confidence in the approximated results) is also starting to border on the problem of redundancy. The overabundance of information, beyond the increased demand for storage space, encumbers the computational process and the assessment of an analysed phenomenon or space, sometimes making it virtually impossible. The problem is not only the redundancy but also the ability to integrate different data [1]. This problem is particularly pronounced during

Article history: received on Mar. 01, 2017; accepted on Oct. 14, 2017; available online on Mar. 26, 2018, DOI: 10.24425/118156.

the space modelling process, in which the high automation of work and minimization of manual intervention is crucial. Certainly, the technologies that relate to these limitations include measurement of laser scanning with ALS (Airborne Laser Scanning) [2, 3], TLS (Terrestrial Laser Scanning) [4–7] MLS (Mobile Laser Scanning) [8] and even optical scanning [9, 10]. With these methods clouds consisting of thousands and even millions of points can be obtained. Depending on the capture method and the recording format, each point is determined by its coordinates. Additional data may characterize the point's colour and its reflectivity. Measurement of cylindrical objects, including silos and tunnels, requires filtration of data in order to evaluate deformations and imperfections. In this case, the Terrestrial Laser Scanning (TLS) method enables to comprehensively analyse the object's geometry. The measurement results can be used to evaluate safety and stability of the examined structures.

Having on mind the laser scanning, the problem of redundancy was mentioned in [11], in the context of selecting an appropriate density of points ensuring a desired accuracy. Another example of controlling too many points is filtering [12, 13].

The use of laser scanning for the purpose of modelling is common [14–16]. This measurement technology can be used [6] for modelling the deformation of a slender-building axis. The nature and definition of tubular objects imposed thinking about their horizontal cross-section, which can be well described by a convex hull. However, the authors' practical analysis of the problem pointed to many lapses in this simplifying assumption. Many objects defined as cylindrical ones have on their surfaces artefacts deforming the nature of the convex hull in analysing their horizontal sections. Another issue is that part of the modelled cylindrical surface is quite often either not visible during the measurement process or its structure does not enable its implementation using the laser technology directly.

Therefore, in this paper, the authors extend the already extensive range of algorithms for the automatic or semiautomatic modelling of cylindrical objects, which have been measured using the laser scanning technology, with the one employing a concave hull or – in general – the alpha-shape (α-shape) [17].

The algorithm is discussed in detail in Section 2. Its applications to numerical simulations of data and real observations are provided in Sections 3 and 4, respectively. The summary and conclusions are presented in Section 5.

2. Method description

Given a finite set of measurement points from the narrow horizontally-oriented section of thickness ΔZ, which are projected onto a horizontal plane, it may look as follows: Fig. 1a.

Assuming the use of a convex hull for the set of projected points shown in Fig. 1, the acquired shape (the outline for this part of the object) would be similar to a rectangle, which would not be consistent with reality. Running the 2D Delaunay triangulation process for the same set, a mesh of triangles shown in Fig. 1b is obtained. On this basis, so-called α-shapes can be generated. An α-shape is a circumferential line which is formed on the basis of leaving only those triangles (obtained from the 2D Delaunay triangulation) for which the distances between the vertices (nodes) are smaller than $2R$ – assumed for a particular α-shape, where R is a radius of the "filtering" circle. A graphical interpretation of this "filtering" of triangles is the creation of a moving circle with a specified radius R on the envelope of the mesh of triangles, and the removal of the edges distant by more than 2R. The effect of such a geometry filter is shown in Fig. 1c. After finding "illegal" outer edge triangles, which have more than one "illegal" edge, these triangles are removed; see: Fig. 1d.

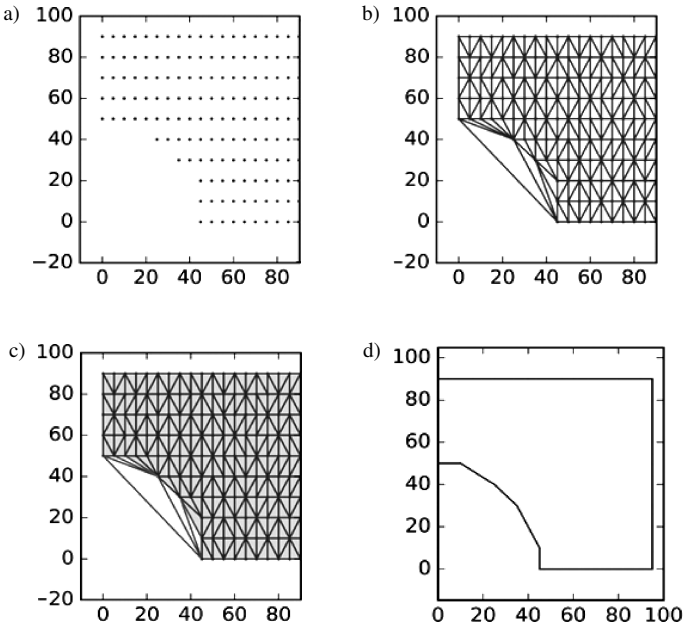

Fig. 1. The theoretical approach to the α-shape: a) an orthogonal projection of points from a set of measured points on a section of thickness ΔZ on a horizontal plane, b) the 2D Delaunay triangulation based on the measured points, c) the indication of edges which do not entirely fit within the defined filtration circle, d) an α-shape obtained for radius R.

3. Implementation of method for simulated data

In order to verify correctness of the assumptions adopted in Section 2, a theoretical model of a classic measurement cylinder with a height of 10 metres and a radius R has been constructed. The R value varied around the nominal 12.00 metre value, with a standard deviation of 0.04 m. This model resembles a standard measurement with the use of laser scanning.

It is assumed that the variability of the object axis (in the vertical direction) is to be assessed at 0.20 metre intervals. Thus, during the construction of a theoretical measuring set (x_{t_i}, y_{t_i}), known changes of the positions of its axes (implicit $x_t = 0$, $y_t = 0$) were introduced for particular sections. The disorder centre of the building (the axis of points) was conditioned by the trigonometric function. For x_{t_i} the disorder was defined by the equation (1) and for y_{t_i} – by the equation (2):

$$dev_{x_{t_i}} = \sin(p_i), \tag{1}$$

$$dev_{y_{t_i}} = \cos(p_i), \tag{2}$$

$$p_i = 0.02\pi z_{t_i} \qquad \text{for } z_{t_i} = [0,\ 10]m, \tag{3}$$

where: p_i – a phase of the centre.

For the entire cylinder, 200,000 points were generated, corresponding to the average density of 212.20 points per square metre. This is a high resolution, assumed only for the theoretical calculation presented in this paper. It means that along axes x and y the distances between points

are about 0.07 m. Changes of the positions of the axes of point subsets are shown in Fig. 2 for XZ and YZ planes, respectively.

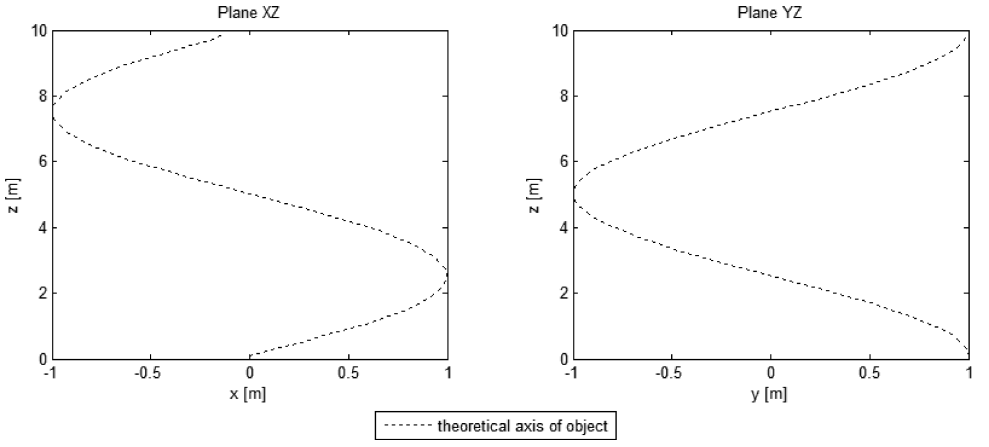

Fig. 2. Changing the position of the theoretical building axis projected on XZ, YZ planes.

The resultant model set of points was divided into sections (subsets), placed between horizontal planes separated by 0.20 metre intervals. For a 10 metre high object, 50 sections were obtained. By using α-shape with a parameter R value equal to 12.00 metres (according to the rough approximation of the silo radius), smoothed boundaries were generated and redundant shape inequalities eliminated – Fig. 3. The parameter R value was chosen according to the rough approximation of the silo radius. This filter radius size is simple to choose, and does not need even a few empirical comparative calculations, but only knowledge of an approximate shape / size of building. The radius value was selected in accordance with the applicable rules related to the accuracy of the location of objects of the 1st accuracy group (Regulation of the Minister of Interior and Administration of 9 November 2011 concerning the technical standards of performance of surveying site and elevation measurements and elaboration and submission of the results of such measurements to the National Surveying and Cartographic Resource Centre; Journal of Laws no. 263, item 1572) and the principles of evaluation of silo and tank structures

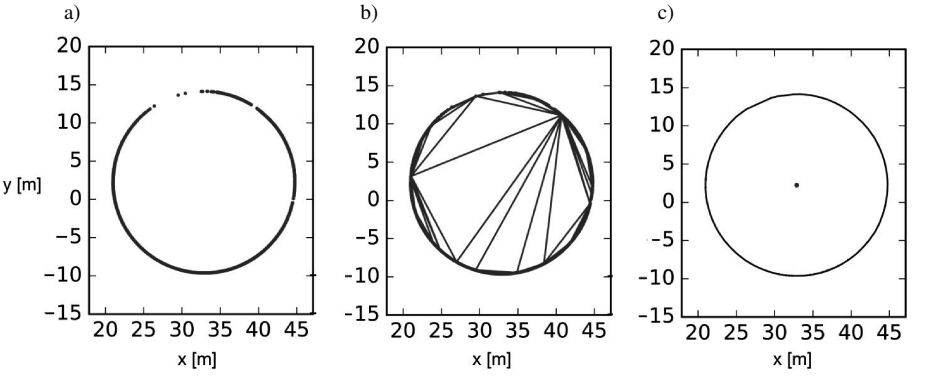

Fig. 3. The stages of approximation of the boundary of cylindrical buildings with the use of α-shape.

adopted in the literature [6, 18, 19]. The centres of alpha shapes s (x_{s_i}, y_{s_i}) were calculated as "centres of gravity" of polygons made of material of uniform density:

$$x_{s_i} = \frac{1}{6A_i} \sum_{j=1}^{N} (X_{V_j} + X_{V_{j+1}})(X_{V_j} Y_{V_{j+1}} - X_{V_{j+1}} Y_{V_j}), \tag{4}$$

$$y_{s_i} = \frac{1}{6A_i} \sum_{j=1}^{N} (Y_{V_j} + Y_{V_{j+1}})(X_{V_j} Y_{V_{j+1}} - X_{V_{j+1}} Y_{V_j}), \tag{5}$$

where:

A – a surface area, X_V, Y_V – coordinates of α-shape vertices,

N – the number of α-shape vertices, i – number of section.

For smoothed boundaries (i.e. polygons), the coordinates of their geometrical centre location were calculated (x_{s_i} and y_{s_i}). They are listed for each level and – together with α-approximations – are presented in Table 1.

Table 1. The list of x, y, z coordinates of building geometrical centres, at different levels, calculated for a polygon resulted from the envelope 2D Delaunay triangulation and α-shape.

z_{t_i} [m]	x_{t_i} [mm]	y_{t_i} [mm]	x_{s_i} [mm]	y_{s_i} [mm]	$v_{x_i} = x_{t_i} - x_{s_i}$ [mm]	$v_{y_i} = y_{t_i} - y_{s_i}$ [mm]	z_{t_i} [m]	x_{t_i} [mm]	y_{t_i} [mm]	x_{s_i} [mm]	y_{s_i} [mm]	$v_{x_i} = x_{t_i} - x_{s_i}$ [mm]	$v_{y_i} = y_{t_i} - y_{s_i}$ [mm]
0.100	1	1000	0	1000	1	0	5.100	−49	−997	0	−1000	−49	3
0.300	128	992	125	992	3	0	5.300	−169	−983	−125	−992	−44	9
0.500	262	962	249	969	13	−6	5.500	−298	−953	−249	−969	−49	16
0.700	376	925	368	930	8	−4	5.700	−411	−912	−368	−930	−43	17
0.900	490	870	482	876	8	−7	5.900	−523	−853	−482	−876	−41	24
1.100	608	789	588	809	20	−20	6.100	−629	−778	−588	−809	−41	31
1.300	706	705	685	729	22	−24	6.300	−719	−694	−685	−729	−35	35
1.500	794	608	771	637	23	−29	6.500	−799	−597	−771	−637	−28	40
1.700	860	510	844	536	15	−26	6.700	−871	−490	−844	−536	−26	46
1.900	920	388	905	426	15	−38	6.900	−925	−379	−905	−426	−21	47
2.100	961	267	951	309	10	−42	7.100	−961	−260	−951	−309	−10	49
2.300	987	140	982	187	4	−47	7.300	−989	−140	−982	−187	−7	47
2.500	999	28	998	63	1	−35	7.500	−996	−14	−998	−63	2	49
2.700	994	−101	998	−63	−4	−38	7.700	−994	111	−998	63	4	49
2.900	969	−233	982	−187	−13	−46	7.900	−969	237	−982	187	13	50
3.100	935	−355	951	−309	−16	−46	8.100	−933	358	−951	309	18	49
3.300	883	−469	905	−426	−22	−43	8.300	−881	471	−905	426	24	45
3.500	817	−571	844	−536	−27	−35	8.500	−812	578	−844	536	32	42
3.700	740	−668	771	−637	−30	−30	8.700	−735	676	−771	637	35	39
3.900	652	−754	685	−729	−33	−25	8.900	−646	763	−685	729	38	34
4.100	549	−833	588	−809	−38	−24	9.100	−543	837	−588	809	45	28
4.300	439	−896	482	−876	−43	−20	9.300	−434	898	−482	876	48	22
4.500	322	−944	368	−930	−47	−14	9.500	−318	947	−368	930	50	17
4.700	201	−976	249	−969	−47	−8	9.700	−196	981	−249	969	53	12
4.900	74	−997	125	−992	−51	−5	9.900	−126	991	−125	992	−1	−1

The standard deviation of axis position determination using α-shape terms of simulated data is obtained according to the formula:

$$\sigma = \pm\sqrt{\frac{\sum_{i=1}^{n}(a_i - \overline{a})^2}{n-1}}, \tag{6}$$

whereas the RMS error is calculated using the following formula:

$$RMSE = \pm\sqrt{\frac{\sum_{i=1}^{n} a_i^2}{n}}, \tag{7}$$

where:

a_i – differences between x_{s_i} and x_{t_i} values (v_{x_i}) or y_{s_i} and y_{t_i} values (v_{y_i}),

n – the number of centres,

$$\overline{a} = \frac{\sum_{i=1}^{n} a_i}{n}. \tag{8}$$

Table 2. Errors of determining centres with the α-shape method for simulated data.

RMSE x	30 mm
RMSE y	32 mm
standard deviation x	30 mm
standard deviation y	32 mm
maximum difference v_{x_i}	53 mm
maximum difference v_{y_i}	49 mm
mean v_{x_i}	−5 mm
mean v_{y_i}	4 mm

A graphical comparison of the theoretical and approximated positions of building axis points projected on XZ, YZ planes respectively are shown in Fig. 4.

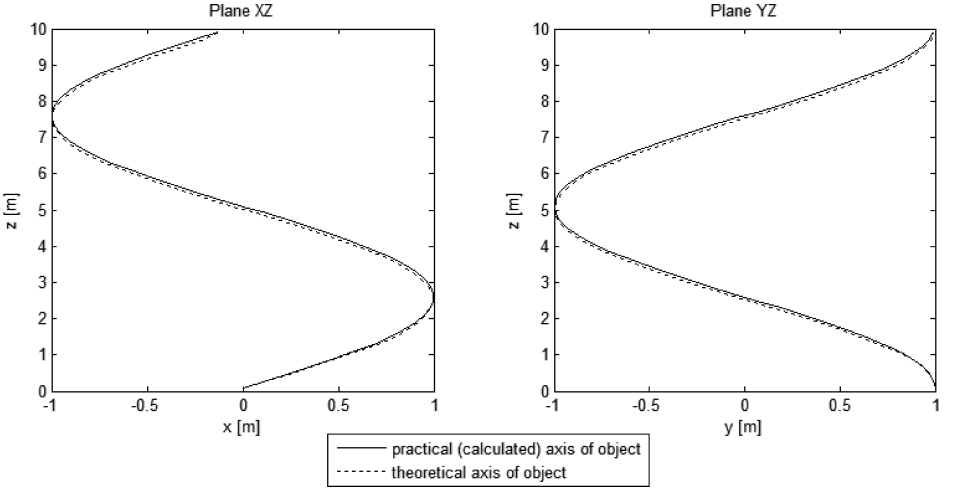

Fig. 4. A graphic comparison of the positions of the axis (theoretical and with α-shape) – XZ and YZ planes.

4. Test of method

The analysed real data were obtained from measurements performed on the COMAL company premises. COMAL is a petroleum products' storage company operating in Gdansk. A detailed description of its tanks and data acquisition process is presented elsewhere [6]. In order to validate the method proposed in this paper, the experimental results (obtained with the circle fitting method) [6] were used. The process of analysing 447,686 point was the same as for the simulated data. An evaluation of the axis obtained with the alpha shape is shown in Fig. 5 (a solid line). The figures include not only the results of the analyses carried out in this paper. The axis determined by the circle fitting method [6] was presented on the same charts with dotted lines. It provides the ability to compare these methods.

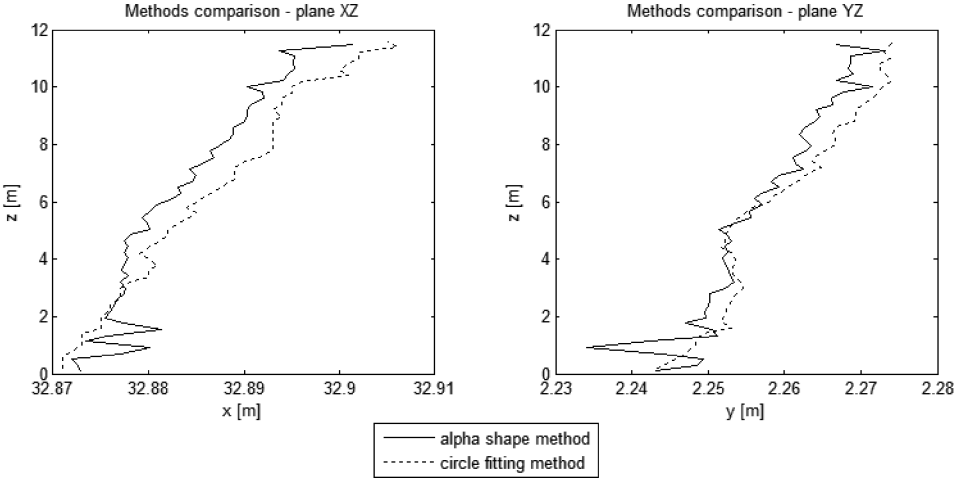

Fig. 5. Determination of the tank axis – comparison of two methods.

Comparing the two methods enabled to determine errors associated with each of them. One set of data has been used as the reference data. The second one contained the comparison data. On this basis, both RMS error (equation (11)) and standard deviation (equation (10)) of one method in relation to the other were calculated. The findings are reported in Table 3. The differences in positions are shown in Fig. 6.

$$\overline{\Delta p} = \frac{\sum_{i=1}^{m} \Delta p_i}{m}, \tag{9}$$

$$\sigma = \pm\sqrt{\frac{\sum_{i=1}^{m} (\Delta p_i - \overline{\Delta p})^2}{m-1}}, \tag{10}$$

where:

m – the number of centres,

Δp_i – a distance (on XY plane) between the centres designated by the α-shape and circle fitting methods

$$RMSE = \pm\sqrt{\frac{\sum_{i=1}^{m} \Delta p_i^2}{m}}. \tag{11}$$

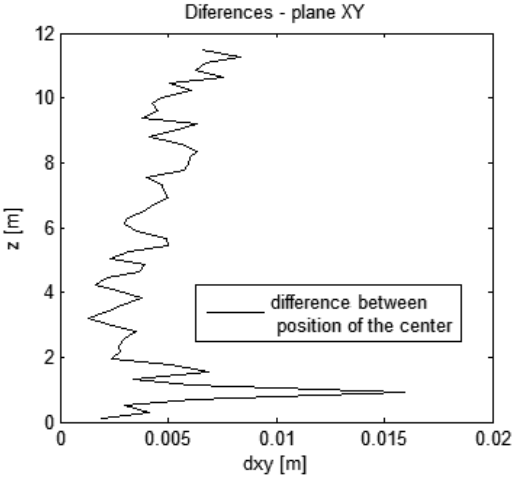

Fig. 6. The differences between the centres designated with different methods – comparison of two methods.

Table 3. The differences between centres determined with the α-shape and circle fitting methods for real data.

standard deviation	2 mm
average residual error	4 mm
RMSE	5 mm

Comparison of the results shows the differences between the methods. These differences are not significant. They may result, among others, from an irregular cross-section shape, roughness of the building or the accuracy of the scan.

Figures 5 and 6 contain several spikes. They appear because of the referenced method of approximation (using ordinary centres) being more general than the evaluated method, giving a possibility of constructing more complicated approximation figures.

The authors used the fitting circles method as the referenced method because of its correct results for cylindrical objects. Unfortunately, using it for more complicated buildings, according to the taken assumptions, is impossible. The proposed method provides the possibility of using it for more complex closed objects and obtaining satisfactory results.

5. Summary

The proposed method of analysing data obtained with the scanning techniques enables to determine the axes of slender buildings, especially of cylindrical tanks, which is presented in this paper. The results, presenting accuracy of the methods based on the analysis of simulated data,

support the conclusion that the method can be widely used. The analysis of practical data led to results similar to those obtained with another method. As a result of comparing the two methods the obtained values of standard deviation, average residual error and RMS error were 2 mm, 4 mm and 5 mm, respectively. The circle fitting method [6] mentioned in the paper enables to designate the centre of a regularly-shaped building with a circular cross-section. However, the 2D Delaunay triangulation and α -shape methods may be used to analyse irregular-shaped slender buildings, even with significant recesses and protrusions. The appropriate use of the R (radius) parameter can resolve these difficulties. Development of this method will make possible its adapting to the work related to the stakeout and modelling structures [20] with a similar cross-section.

References

[1] Amirian, P., Basiri, A., Winstanley, A. (2013). Efficient Online Sharing of Geospatial Big Data Using NoSQL XML Databases. *2013 Fourth International Conference on Computing for Geospatial Research and Application*, 152–152.

[2] Janowski, A., Rapiński, J. (2013). M-split estimation in laser scanning data modeling. *J. Indian Soc. Remote Sens.*, 41(1), 15–19.

[3] Tomljenovic, I., Rousell, A. (2014). Influence of point cloud density on the results of automated Object-Based building extraction from ALS data. *AGILE Conference Castellon*.

[4] Burdziakowski, P., Janowski, A., Kholodkov, A, *et al.* (2015). Maritime laser scanning as the source for spatial data. *Pol. Mar. Res*., 22(4), 9–14, 2015.

[5] Janowski, A., Nagrodzka-Godycka, K., Szulwic, J., Ziółkowski, P. (2016). Remote sensing and photogrammetry techniques in diagnostics of concrete structures. *Comput. Concr.*, 18(3), 405–420.

[6] Janowski, A., Szulwic, J., Zuk, M. (2015). 3D modelling of liquid fuels base infrastructure for the purpose of visualization and geometrical analysis. *15th International Multidisciplinary Scientific GeoConference SGEM 2015, www.sgem.org, SGEM2015 Conference Proc.*, 1, 753–764.

[7] Bobkowska, K., Inglot, A., Mikusova, M. *et al*. (2017). Implementation of spatial information for monitoring and analysis of the area around the port using laser scanning techniques. *Pol. Mar. Res*., 24(SI1), 10–15.

[8] Szulwic, J., Tysiac, P., Wojtowicz, A. (2016). Coastal cliffs monitoring and prediction of displacements using terrestial laser scanning. *Baltic Geodetic Congress (Geomatics)*, 61–66.

[9] Bobkowska, K., Janowski, A., Przyborski, M., Szulwic, J. (2016). Analysis of high resolution clouds of points as a source of biometric data. *Baltic Geodetic Congress (Geomatics)*, 15–21.

[10] Majchrowski, R., Grzelka, M., Wieczorowski, M., Sadowski, Ł., Gapiński, B. (2015). Large area concrete surface topography measurements using optical 3D scanner. *Metrol. Meas. Syst.*, 22(4), 565–576.

[11] Liu, X., Zhang, Z. (2008). LiDAR data reduction for efficient and high quality DEM generation. *International Archives of the Photogrammetry, Remote Sensing and Spatial Information Sciences*, 37, 173–178.

[12] Lin, X., Zhang, J. (2014). Segmentation-based filtering of airborne LiDAR point clouds by progressive densification of terrain segments. *Remote Sens.*, 6(2), 1294–1326.

[13] Zhu, N., Jia, Y., Luo, L. (2016). Tunnel point cloud filtering method based on elliptic cylindrical model. *International Archives of the Photogrammetry, Remote Sensing & Spatial Information Sciences*, 41(B1), 735–740.

[14] Huang, H., Brenner, C., Sester, M. (2013). A generative statistical approach to automatic 3D building roof reconstruction from laser scanning data. *ISPRS J. Photogramm. Remote Sens*., 79, 29–43.

[15] Xiong, X., Adan, A., Akinci, B., Huber, D. (2013). Automatic creation of semantically rich 3D building models from laser scanner data. *Autom. Constr*., 31, 325–337.

[16] Zhu, L., Hyyppa, J. (2014). The Use of Airborne and Mobile Laser Scanning for Modeling Railway Environments in 3D. *Remote Sens*., 6(4), 3075–3100.

[17] Akkiraju, N., Edelsbrunner, H., Facello, M., Fu, P., Mucke, E.P., Varela, C. (1995). Alpha shapes definition and softwar. *Internat.Comput. Geom. Software Workshop*.

[18] Niedostatkiewicz, M., Tejchman, J., Chaniecki, Z., *et al.* (2009). Determination of bulk solid concentration changes during granular flow in a model silo with ECT sensors. *Chemical Engineering Science*, 64(1), 20–30.

[19] Wojcik, M., Sondej, M., Rejowski, K., *et al*. (2017). Full-scale experiments on wheat flow in steel silo composed of corrugated walls and columns. *Powder Technology*, 311, 537–555.

[20] Rapinski, J., Janowski, A. (2016). Algorithm for Staking Out Interior Elements of the Wind Turbine Monopile. *J. Surv. Eng*., 04016029.